Metastable trapping of low-energy positrons by cubane: A computational experiment

F. A. Gianturco*
Department of Chemistry, University of Rome "La Sapienza" and INFM, Piazzale A. Moro 5, 00185 Rome, Italy

P. Nichols
Department of Chemistry, University of New Orleans, New Orleans, Louisiana 70148, USA

T. L. Gibson
Department of Physics, Texas Tech University, P. O. Box 4180, Lubbock, Texas 79409-1051, USA

R. R. Lucchese
Department of Chemistry, Texas A&M University, College Station, Texas 77843-3255, USA
(Received 11 April 2005; published 21 September 2005)

Quantum-mechanical calculations of low-energy collisions of positrons with cubane (C_8H_8) molecules are carried out using a model interaction potential and solving the corresponding scattering equations. The possible presence of low-energy resonances is analyzed in detail and one of them is found to reside largely inside the carbon frame of the cubane. The consequences of this finding are discussed and analyzed.

DOI: 10.1103/PhysRevA.72.032724 PACS number(s): 34.10.+x, 36.10.Dr

I. INTRODUCTION

The study of low-energy scattering of positrons from molecular gases and solids has received a great deal of attention in the past few years, both experimentally and theoretically [1–3]. This interest has been prompted by the broad range of applications that have been found for thermal or subthermal positron beams. Such studies have been facilitated by the marked improvements in the technology that have provided better sources and better beam capabilities [4] and by the corresponding advances in the computational models which can describe positron processes involving large molecular systems [5]. Due to the presence of a much higher density of internal states in molecular systems, molecules provide a more efficient environment than atoms for slowing down positrons. Furthermore, the positron-molecule interaction has a richer variety of possible channels compared to when electrons are used as probes of molecular systems. For example, there is the possibility of forming positronium (Ps) compounds which suggests that molecular ions can be prepared in a "gentle" manner, i.e., with fairly little internal excitation of the final cations, and therefore could be experimentally manipulated for longer times than those formed by electron impact ionization techniques. Additionally, the particle-antiparticle decay channel, whereby the pick-off of a bound electron by the positron leads to the emission of two γ photons and again to cation formation in a molecular gas, is also an additional channel in the case of positron projectiles which becomes very interesting in a molecular environment [3].

The analogy with electron scattering can be extended to complex molecular systems, e.g., benzene or sulfur hexafluoride, where the experiments and the calculations for low-energy collision processes [6,7] have revealed a great variety of resonant processes which cause marked enhancement in the corresponding elastic and inelastic cross sections and which also dominate the subsequent "unimolecular"-type decay with fragmentation of the initial species and frequent electron attachment to one of the fragments (for a recent review see, e.g., Ref. [8]). In such instances, in fact, the likely existence of precursor states that correspond to electron trapping by dynamical angular momentum effects (shape resonances) has been suggested in many cases [5–7] and has provided a useful rationalization of a broad variety of experiments involving low-energy electrons [9].

Because of the differences which exist, at the nanoscopic level, between the types of forces which drive the above-mentioned processes with electrons and the similar dynamics with slow positrons, it is certainly intriguing to investigate how many of the possible outcomes from positron scattering off the more complicated polyatomic gases could be either explained, or predicted, by considering the dynamical trapping at low energies by the molecule. In recent studies on simple polyatomics, we have shown that positrons form virtual states with vibrationally excited molecular species [10,11] and that such states have marked consequences for the features associated with, for example, the annihilation parameters of the ambient gas.

In the present computational analysis, therefore, we investigate whether a realistic model of the interaction forces between e^+ and the cage structure of the cubane molecule depicted in Fig. 1 can lead to the possible trapping of a positron by the molecule and indicate where within that structure the positron density will be localized. In the next section, we outline our theoretical and computational model while we present our results in Sec. III. Our present conclusions are given in Sec. IV.

*Corresponding author. Email address: fa.gianturco@caspur.it; FAX: +39-06-49913305.

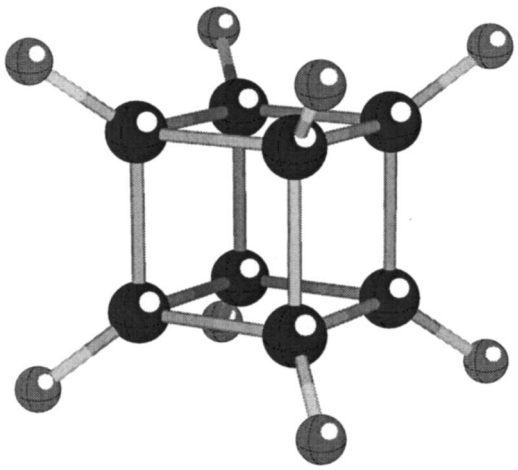

FIG. 1. Three-dimensional view of the equilibrium structure of cubane, showing the atoms of the carbon cage and the outer hydrogen atoms.

II. THE THEORETICAL MODEL

In this study, we represent the interaction potential between the impinging positron and the molecular target with a local form. The potential contains contributions from the electrostatic interaction of e^+ with the molecular nuclei (kept fixed at their equilibrium geometry) and the bound molecular electrons plus the correlation effects from the short-range dynamical couplings between the bound electrons and the positron, $V_{\rm corr}$, that evolve for the long-range region of large e^+-molecule distances into the dipole polarization potential $V_{\rm pol}$. We shall consider two different correlation-polarization potentials,

$$V_{\rm pcp} = V_{\rm corr} + V_{\rm pol}, \tag{1}$$

which have been used for polyatomic targets, and the corresponding differences in scattering attributes.

A. Single center expansion equations

In our approach, any three-dimensional function, being either one of the bound state orbitals $\phi_i(\mathbf{r})$ for one of the N bound electrons or the scattering wave function $\psi(\mathbf{r}_p)$ describing the impinging positron, is written as a single-center expansion (SCE) located at the center of mass of the molecule,

$$\phi_i^{p_i\mu_i}(\mathbf{r}) = \frac{1}{r}\sum_{l,h} u_{ilh}^{p_i\mu_i}(r) X_{lh}^{p_i\mu_i}(\hat{r}), \tag{2}$$

$$\psi^{p\mu}(\mathbf{r}_p) = \frac{1}{r_p}\sum_{l,h} \psi_{lh}^{p\mu}(r_p) X_{lh}^{p\mu}(\hat{r}_p), \tag{3}$$

where i labels a specific, multicenter occupied orbital, which belongs to a specific irreducible representation (IR) of the point group of the molecule. The index p labels a relevant IR and μ indicates one of its components. The index h labels a specific angular basis function for a given partial wave l, used within the μth component of the pth IR. The symmetry-adapted angular functions in Eqs. (2) and (3) are defined by

$$X_{lh}^{p\mu}(\hat{r}) = \sum_m b_{lmh}^{p\mu} Y_{lm}(\hat{r}). \tag{4}$$

The details about the computation of the transformation matrices $b_{lmh}^{p\mu}$ have been given before and will not be repeated here [12].

We assume that the interaction potential can be written in a local form $V_{\rm loc}(\mathbf{r}_p)$ (here the static and correlation-polarization potentials) for a positron-molecule collision. The SCE then results in the following set of radial differential equations:

$$\left[\frac{d^2}{dr_p^2} - \frac{l_i(l_i+1)}{r_p^2} + k^2\right]\psi_{ij}^{p\mu}(r_p) = 2\sum_k \left[V_{{\rm loc},ik}(r_p)\psi_{kj}^{p\mu}(r_p)\right], \tag{5}$$

where indices i,j,k represent pairs of angular channel indices (l,h).

The required full interaction potential in Eq. (5) can be written as

$$V_{\rm loc}(\mathbf{r}_p) = V_{\rm st}(\mathbf{r}_p) + V_{\rm pcp}(\mathbf{r}_p), \tag{6}$$

where $V_{\rm st}(\mathbf{r}_p)$ is the familiar static potential between the impinging positron and the target (bound electrons+nuclei) and $V_{\rm pcp}$ describes the short-range and long-range correlation-polarization interaction forces [5]. The SCE equations can then be solved using standard methods for solving ordinary differential equations [13].

A rigorous approach for the inclusion of positron-electron correlation is to use an extensive configuration-interaction expansion of the target electronic wave function over a suitable set of excited electronic configurations and further improvement of the wave function by adding Hylleraas-type functions which can describe the positron wave function within the physical space of the target electronic charge distribution [14]. Such expansions, however, are markedly energy-dependent, and usually converge too slowly to be a useful tool for a general implementation with complex molecular targets, where truncated expansions need to be very large before they begin to be realistic in describing correlation effects [15,16].

As a less computationally intensive alternative, we have developed global models of the correlation-polarization effects which do not depend on empirical parameters but can be implemented via a simplified, local representation of the correlation-polarization interactions, $V_{\rm pcp}(\mathbf{r}_p)$.

B. The distributed positron model

One model correlation-polarization potential we have used to $V_{\rm pcp}$ in Eq. (6) is the distributed positron model (DPM) potential, $V_{\rm pcp}^{\rm DPM}$ [17,18]. The form adopted here for the $V_{\rm pcp}^{\rm DPM}$ is based on a modification of the adiabatic polarization effect which makes use of quantum chemistry technology to provide a variational estimate of the polarization potential. In the adiabatic approximation to that potential, in fact, the positron is treated as an additional "nucleus" (a point charge of +1) fixed at location $\mathbf{r}_p$ with respect to the

center of mass of the atomic or molecular target. The target electronic orbitals are allowed to relax fully in the presence of this fixed additional charge and the energy lowering due to the distortion is recorded. This energy lowering represents the adiabatic polarization potential at one point in space. Of course, in order to represent fully the spatial dependence of this interaction, many such points must be computed.

However, due to nonadiabatic and short-range correlation effects, e.g., virtual Ps formation, the adiabatic approximation can overestimate the strength of the polarization potential for smaller values of r_p, where the positron has penetrated the target electronic cloud. The present model corrects for this by treating the positron as a "smeared out" distribution of charge rather than as a point charge. If the scattering particle really were an additional point charge, then the dominant short-range correlation effect would be virtual hydrogen atom formation into ground and excited states, and the δ-function distribution of positive charge at the center of mass would be correct. But, for a Ps atom, the positive charge is not localized at the center of mass, and to mimic this effect in computing the polarization potential we represent the positron as a spherically symmetric distribution of charge. This leads to a polarization potential that more closely reflects the correct physics and that smoothly reduces to the expected result for larger values of r_p without any need to select a crossover distance or make additional ad hoc corrections.

Within the DPM one can, in principle, choose any reasonable distribution that approximates the positive charge for virtual Ps embedded in the near-target environment. However, it is our experience that the results are fairly sensitive to the effective size of the distribution. In our initial proof-of-concept studies [17,18], we selected two very simple uniform spherical charge distributions based on the radius of the positive charge (with respect to the Ps center of mass) of 1.0 bohr, the maximum in the radial distribution, and the average radius of 1.5 bohr. Both cases provided scattering results that were in significantly better agreement with measured values than those obtained with the adiabatic polarization potential, with the larger radius distribution being better for molecular targets. To implement the model for polyatomic target molecules [19,20], we construct the positron charge distribution from a 1s STO-3G basis function with the tighter Slater exponent of $\xi=1.24$ that is recommended [21] for a molecular environment. The STO-3G distribution yields scattering results close to that of the larger uniform spherical distribution, but is much easier to implement numerically. Once the $V_{\mathrm{pcp}}^{\mathrm{DPM}}$ potential is calculated, it is combined with the static potential to yield the total local interaction potential of Eq. (6).

Subsequent to our development of the DPM to account for nonadiabatic polarization effects in positron-molecule scattering, a somewhat similar scheme was proposed by Bouferguene *et al.* [23] for low-energy electron-H_2 collisions in which the polarization interaction is computed by replacing the impinging electron with a spherical Gaussian distribution of charge -1. Like the DPM for positron scattering, this has the effect of reducing the overestimation of the adiabatic potential near the target and can be very efficiently implemented within a quantum chemistry framework.

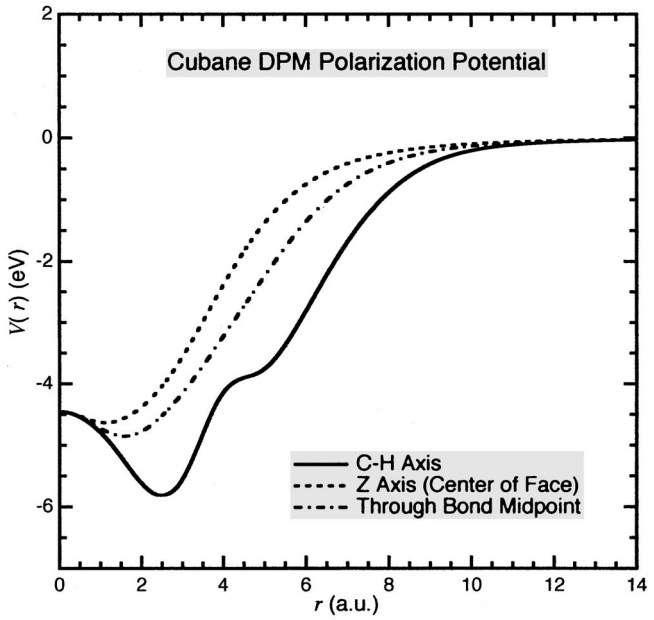

FIG. 2. Computed correlation-polarization potential using the DPM model, $V_{\mathrm{pcp}}^{\mathrm{DPM}}$, shown along three different directions.

However, for electron scattering, the overestimation of the adiabatic polarization potential arises from an increase in the local kinetic energy of the scattering electron when near the target [22] to a value that invalidates the adiabatic assumption that the rapidly moving target electrons adjust fully to the presence of a slow projectile electron. Thus, rather than a single fixed distribution, Bouferguene *et al.* [23] found it necessary to use a distribution that varies with the distance of the scattering electron from the molecular center of mass and involves a semiempirical parameter. In extending this method to electron-N_2 scattering, Feng *et al.* [24] had to introduce additional ad hoc dependences on the orientation of the target nuclei with respect to the projectile and on the internuclear separation distance.

In contrast, we have been able to obtain good agreement with various measured positron-molecule scattering results within the DPM using essentially the same procedure (i.e., without needing to adjust for details of the target molecule) on a variety of systems [17–20] as diverse as H_2 and SF_6. This past success is the chief motivation for including the DPM in the current study.

To implement the model for polyatomic target molecules [19,20], we construct the charge distribution from a 1s STO-3G basis function with Slater exponent $\xi=1.24$. Once the $V_{\mathrm{pcp}}^{\mathrm{DPM}}$ potential is calculated, it is combined with the static potential to yield the total local interaction potential of Eq. (6).

C. The DFT correlation-polarization model

A second model for V_{pcp} is the $V_{\mathrm{pcp}}^{\mathrm{DFT}}$ potential, which has been applied to positron scattering earlier [25] and is based on the correlation energy $\varepsilon^{e\text{-}p}$ of a localized positron in an electron gas. The quantity $\varepsilon^{e\text{-}p}$ was originally derived by Arponen and Pajanne [26,27] from the theory that the incoming

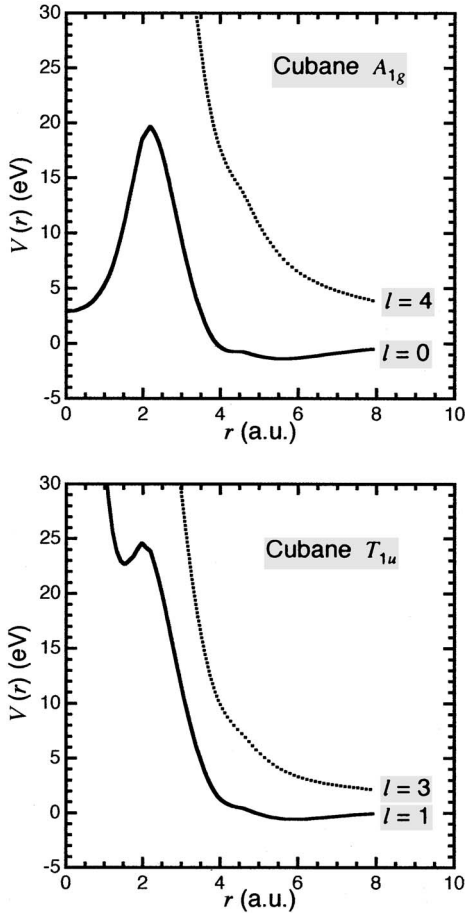

FIG. 3. Computed dominant adiabatic potentials for positron scattering from cubane with the A_{1g} (upper panel) and T_{1u} (lower panel) IR's.

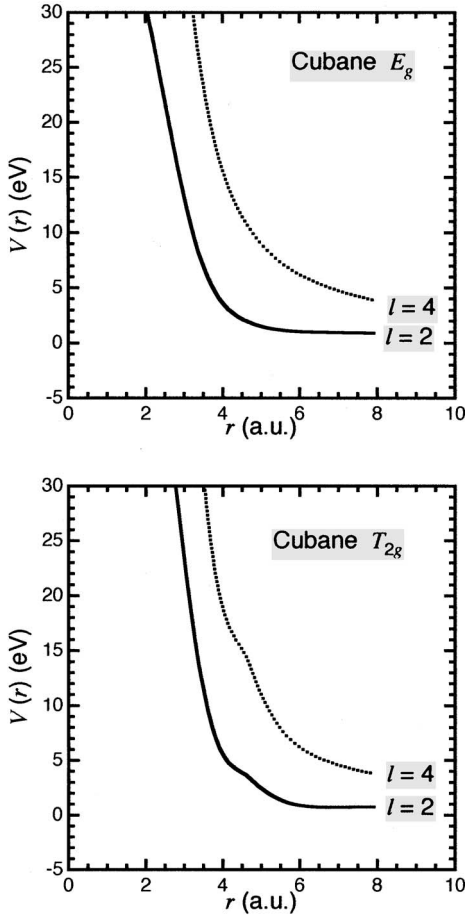

FIG. 4. Same as in Fig. 3 but for the E_g (upper panel) and T_{2g} (lower panel) IR's of the octahedral symmetry of the scattering potential.

positron is assumed to be a charged impurity at each fixed distance $\mathbf{r}_p$ in a homogeneous electron gas, which is in turn treated as a set of interacting bosons which represent the collective excitations provided by the random-phase approximation. Based on their work, Boronski and Nieminen [28] gave the interpolation formulae of $\varepsilon^{e\text{-}p}$ over the entire range of the density parameter r_s which satisfies the relationship of $\frac{4}{3}\pi r_s^3 \rho(\mathbf{r}) = 1$. The relationship between the short-range correlation potential, V_{corr}, and $\varepsilon^{e\text{-}p}$, which is consistent with the local-density approximation and a variational principle for a total collision system with the size of the target, is given by [29]

$$V_{\text{corr}}^{\text{DFT}}(\mathbf{r}_p) = \frac{d}{d\rho}\{\rho(\mathbf{r}_p)\varepsilon^{e-p}[\rho(\mathbf{r}_p)]\}, \tag{7}$$

where ρ denotes the undistorted electronic density of the target. This quantity provides the probability for finding any of the electrons near the impinging positron.

The $V_{\text{corr}}^{\text{DFT}}$ potential, however, does not have the correct asymptotic form as $r_p \to \infty$, which is important for low-energy scattering. We note that the asymptotic form of the interaction is independent of the sign of the impinging charged particle and, in its simpler spherical form, is given by the well-known second-order perturbation expansion formula (in atomic units),

$$V_{\text{pol}}(r_p) \underset{r_p \to \infty}{\sim} \sum_{l=1}^{\infty} -\frac{\alpha_l}{2r_p^{2l+2}}, \tag{8}$$

where r_p represents the distance from the center of mass of the molecule, and α_l are the multipolar static polarizabilities of the molecule. In most cases, only the lowest order is kept in the expansion above, and therefore the target distortion is viewed as chiefly resulting from the induced dipole contribution with the molecular dipole polarizability as its coefficient. The drawback of the above expansion, however, is that it fails to represent correctly the true short-range behavior of the full interaction and does not contain any contributions from dynamic correlation. Therefore, in order to correct for such failures, one needs to model the dynamical correlation effects that dominate the short-range behavior by a potential such as $V_{\text{corr}}^{\text{DFT}}$ given in Eq. (7).

We therefore describe the full $V_{\text{pcp}}(\mathbf{r}_p)$ interaction as given by two distinct contributions which are connected at a distance, r_p^c,

$$V_{\text{pcp}}^{\text{DFT}}(\mathbf{r}_p) = V_{\text{corr}}^{\text{DFT}}(\mathbf{r}_p) \quad \text{for } r_p < r_p^c,$$

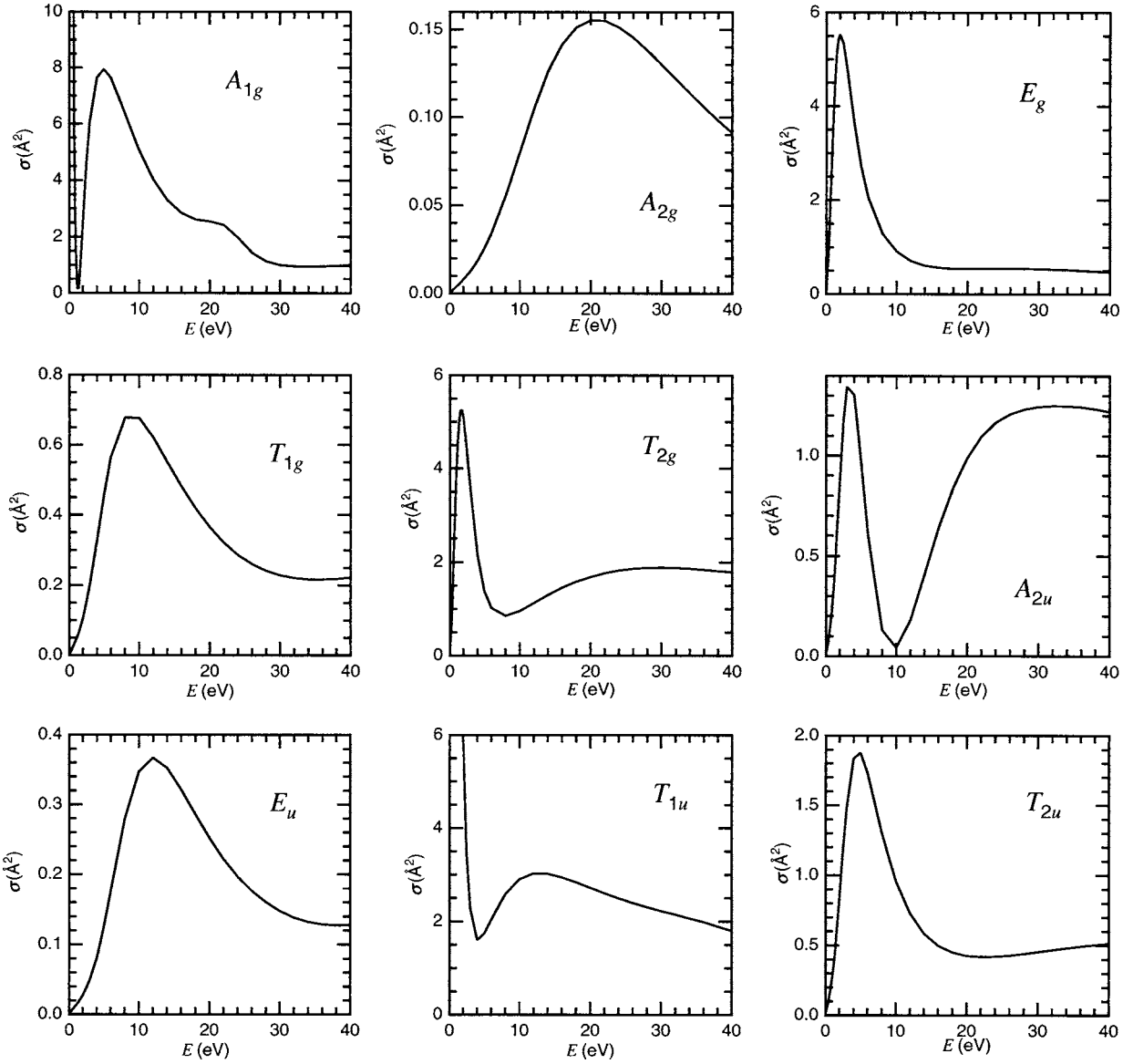

FIG. 5. Computed partial cross sections for all the IR's that make a significant contribution to the total elastic cross sections.

$$= V_{\mathrm{pol}}(\mathbf{r}_p) \quad \text{for } r_p > r_p^c. \tag{9}$$

In the present case, the value for r_p^c is around 4.1 a.u.

The total local interaction potential, $V_{\mathrm{loc}}^{\mathrm{DFT}}$, as defined in Eq. (6), is then given by the sum of the exact static interaction between the impinging positron and the components of the molecular target, V_{st} (for detail forms, see, for example, [12]), and the $V_{\mathrm{pcp}}^{\mathrm{DFT}}$.

It is difficult at this stage to decide which of the two models is likely to be more realistic. The past record of the DFT modeling on polyatomic targets has been more extensive because it is easier to generate in terms of computational cost and has provided thus far good accord with available experiments (e.g., see Refs. [10,11]). On the other hand, the DPM approach is physically more appealing and is being tested increasingly more often with available experiments with reasonable success (e.g., see Refs. [19,20]).

III. RESULTS

The calculations were carried out largely following the numerical details already reported in our previous work on cubane [9]. The molecular structure was taken at its equilibrium geometry of the octahedral structure, using 1.078 Å for the eight C—H bonds and 1.557 Å for the twelve C—C bonds. A pictorial view of the 3D structure is shown for clarity in Fig. 1.

The single-determinant (SD) electronic structure calculations were carried out, as in Ref. [9], using a cc-pVTZ expansion, producing a spherical polarizability of 70.321 a.u.[3]. The anisotropic contributions to the long-range potential in Eq. (9) were generated by equally partitioning that value over the eight carbon centers and then expanding the overall polarization potential over the center of mass of the above structure. The Hartree-Fock (HF) orbitals were also expanded up to $l_{\mathrm{max}}=40$ multipolar terms and the ensuing static and correlation contributions to Eq. (6) were expanded up to

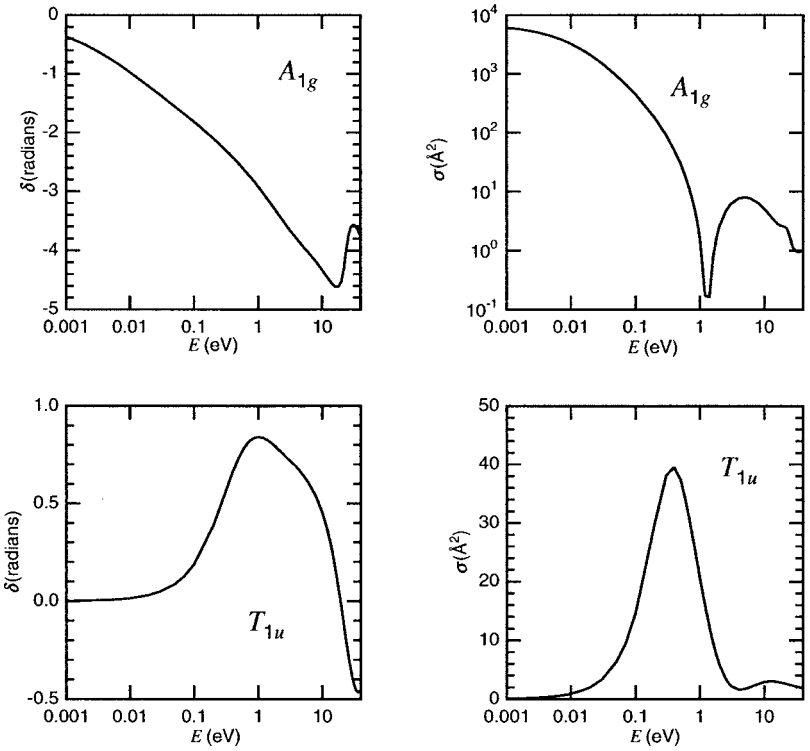

FIG. 6. Computed eigenphase sum and cross sections below 10 eV for the A_{1g} and T_{1u} partial contributions.

$\lambda_{max}=80$. The range of radial integration depended on the collision energy considered and went from about 95 a.u. at the higher collision energy of 20–40 eV to more than 10^3 a.u. for the lower energies of a few meV.

The chief aim of the present study is to see if the simulation of positron scattering from such a cage structure could lead to the presence of trapped, metastable positron states *inside* the carbon network because of the special interplay of attractive-repulsive contributions of the full interaction with this molecule. Our earlier study on the C_{60} carbon cage [5] has indeed suggested that such resonant states exist in the low-energy region, due to barrier trapping generated by the Coulomb potential of the carbon nuclei forming the fullerene structure. It would be of interest to see if the present, smaller, cage structure could lead to a similar effect. The spatial location of the carbon atoms from the center of mass is, in this case, at about 2.0 a.u. and we shall therefore see that the overall size of the present "cage" plays a significant role in the possible trapping of a positron.

In Fig. 2, we report the behavior of our computed $V_{\rm pcp}^{\rm DPM}$ potential along three distinct directions of approach to the target molecule. It is interesting to note that, as expected, the strongest attractive well occurs as the impinging projectile follows the C—H bond and therefore we see a marked local correlation distortion of the hydrogen atom around 5 a.u. followed by the stronger carbon atom correlation contribution with its maximum effect just below 3.0 a.u. On the other hand, the other two directions of approach, where no atomic centers are encountered by the impinging positron, clearly show only the long-range attractive features of the large molecular polarizability of the system that goes to a constant value near the center of the cage.

A more transparent way of analyzing the spatial features of the positron-molecule interaction, especially in the case of highly symmetric systems as in the present instance, is to employ an adiabatic angular basis set expansion of the form

$$Z_k^{p\mu}(\mathbf{r}_p)=\sum_{hl} X_{hl}^{p\mu}(\hat{r}_p)C_{k,hl}(r_p), \tag{10}$$

where the expansion coefficients $C_{k,hl}(r_p)$ are given by a matrix eigenvalue equation

$$\sum_{hl} V_{hl}^{h'l'}(r_p)C_{k,hl}(r_p)=V_k(r_p)C_{k,h'l'}(r_p). \tag{11}$$

The adiabatic eigenvalues V_k therefore depend on the positron-molecule distance and provide a set of adiabatic potentials for each irreducible representation (IR) of the molecular point group. The nonadiabatic coupling terms can be included when the coupled radial equations are solved (see, for details, our earlier work [30–32]) leading to the same results as would be obtained if one solved the usual SCE equations. The adiabatic potentials can provide a fairly compact description of the dominant features of the positron-molecule interaction.

Figures 3 and 4 report the dominant multipolar components for the adiabatic representations of e^+-cubane interaction for four of the dominant IR's associated with the equilibrium geometry, which has octahedral symmetry.

The calculations reported in the two figures clearly show the dominant partial waves, which are active within the range of energies of our present study, i.e., roughly the region from threshold up to about 30 eV. The following considerations could be made by inspecting the potential features reported there.

(i) Essentially all adiabatic potentials turn out to be dominated by repulsive forces (nuclear static contributions plus centrifugal terms) as the positron approaches the center of

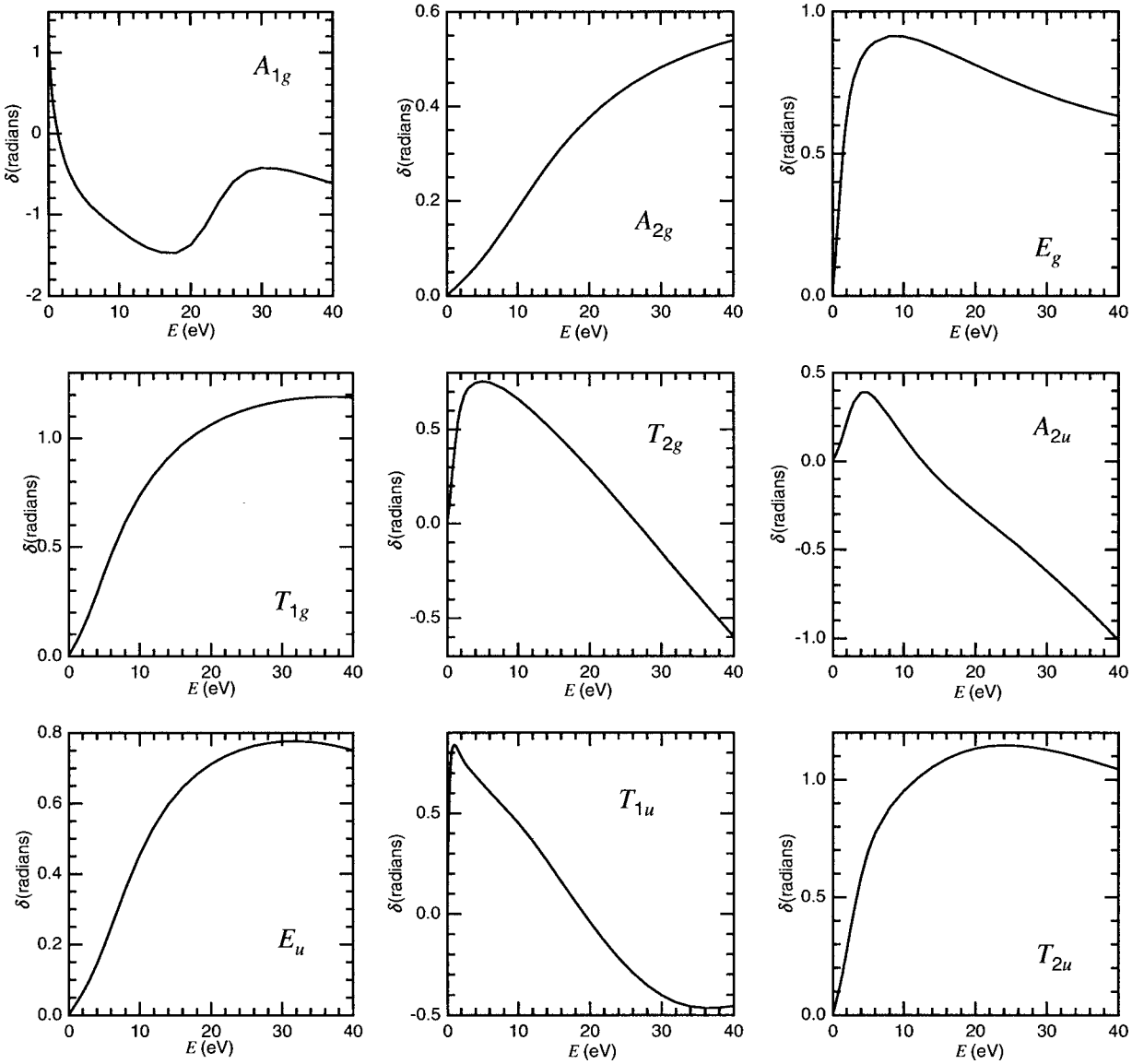

FIG. 7. Computed eigenphase sums for the same symmetry contributions to the cross section reported in Fig. 5.

the cage, with only a very weak indication of long-range attractive features clearly located outside the carbon cage.

(ii) The totally symmetric component A_{1g} is the only adiabatic interaction with an *s*-wave contribution which gives rise to a clear barrier at the boundary of the carbon atom network. This is obviously not a dynamical effect from angular momentum conservation but rather a feature related to the spatial properties of the full interaction that is a balance of the attractive V_{pcp} potential with the strongly repulsive V_{st} interaction of Eq. (6).

We therefore expect that the A_{1g} symmetry component might be the most likely contribution to the total elastic cross section which could provide evidence for metastable trapping of low-energy positrons by the carbon cage of cubane.

In Fig. 5, we report all the computed components of the total elastic (rotationally summed) cross sections using the $V_{\mathrm{pcp}}^{\mathrm{DPM}}$ interaction described in the previous section. It is interesting to see that the largest cross-section contributions come, at low energies, from the T_{1u}, T_{2g}, E_g, and A_{1g} components and that there are several cross-section peaks over the energy range we have examined that also correspond to a marked rising behavior in their eigenphase sums, as discussed later. The most notable indicators of resonant behavior can be seen from the strong peaks, in Fig. 6, of the A_{1g} and T_{1u} cross sections which correspond to steady and strong increases (around the same energies) of their corresponding eigenphase sums. They further show, at such energies, poles of the *S* matrix in the complex plane, from which resonance properties can be extracted.

To analyze such components in greater detail, we report in Fig. 6 the low-energy behavior of the A_{1g} and T_{1u} contributions, showing in the left panels the eigenphase sums and in the right panels the corresponding cross sections. The following considerations could be made.

(i) The partial cross section for the A_{1g} contribution is finite and large at zero energy and falls monotonically down to the high-energy resonance, while the structure seen at low

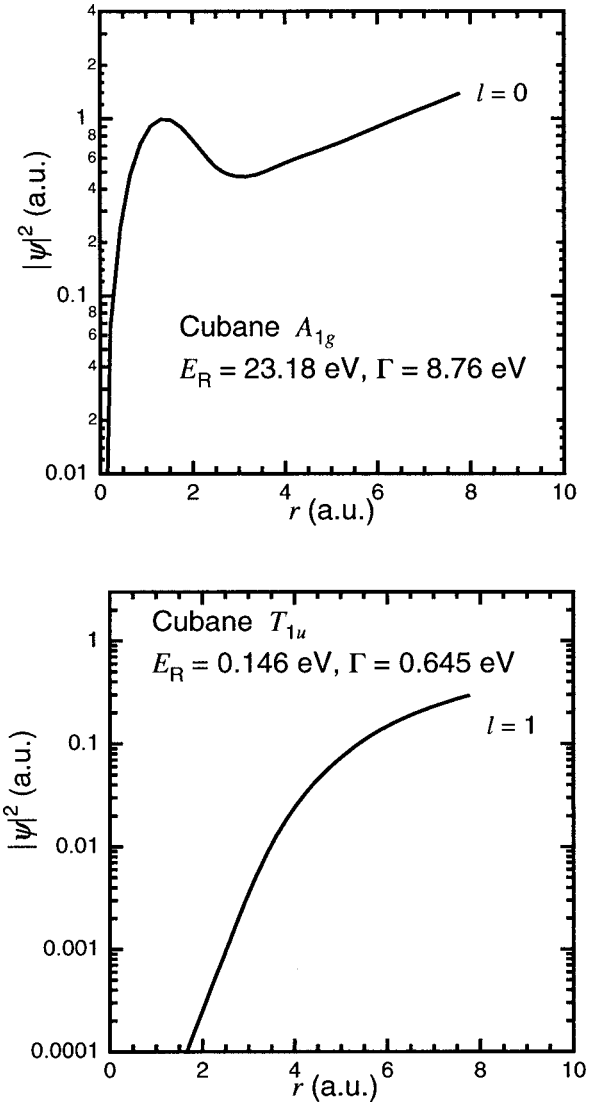

FIG. 8. Computed resonant wave functions for the two S-matrix poles of A_{1g} (upper) and T_{1u} (lower panel) symmetries. Only the dominant partial-wave components are shown.

energy in its cross section is due to the eigenphase sum going through a multiple of π around 1 eV.

(ii) By analyzing the low-energy behavior of the dominant $l=0$ phase shift (eigenphase sum), one obtains the corresponding scattering length of 43.62 bohr. Since it is a positive quantity, there is no virtual state for positron scattering at vanishing collision energies.

(iii) The T_{1u} component shows a marked increase of the eigenphase sum around 1 eV and a corresponding increase of the cross section. As we shall show later on, it corresponds to an "above-the-barrier" resonant behavior with negligible positron localization.

The results of the eigenphase sum calculations for all the contributing partial symmetries are shown by Fig. 7.

The corresponding scattering wave functions are shown in Fig. 8, where we report the dominant component of the A_{1g} resonance in the upper panel and the dominant partial wave for the T_{1u} resonance in the lower panel. The results of this figure are rather interesting in that they clearly show the

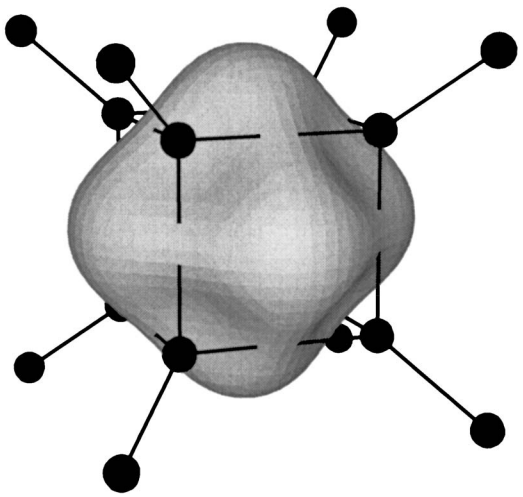

FIG. 9. Three-dimensional view of the A_{1g} resonant orbital with superimposed carbon cage structure of cubane.

presence of an e^+-C_8H_8 complex with a strong amplitude contribution *inside* the C cage and supported at around 23 eV by the potential barrier seen in Fig. 3. One also sees, however, that the corresponding widths from our fixed-nuclei calculation are really very broad. Although one should expect that the inclusion of nuclear dynamics may markedly modify the features of this metastable complex, it is difficult to imagine that such a large amount of excess energy could be efficiently transferred to the carbon cage without also opening up molecular breakup channels.

A pictorial, three-dimensional view of the corresponding resonant orbital is reported in Fig. 9, where the carbon-hydrogen cage structure is shown with the wave function: it is clear from the results presented in Figs. 8 and 9 that the resonant state does correspond to trapping the positron inside the cage, although both width and energy position do not cause this resonance to be physically very likely to occur because of the large amount of positive energy which needs to be disposed of during the very short lifetime of the metastable state.

The low-energy resonance observed for the T_{1u} symmetry (lower panel of Fig. 8) is, on the other hand, much narrower and corresponds to a longer lifetime for the trapped positron. The resonant wave function shown in that figure, however, indicates this state to be dominated by p-wave dynamical trapping of the scattered positron well outside the carbon cage. It is therefore seen as a very diffuse shape resonance with the positron density distributed around the cage structure and well outside it. As discussed before, since we are dealing with a resonance state above the barrier, the corresponding scattering wave function is still very diffuse and will be very difficult to represent as localized within the carbon cage structure.

In the upper panels of Fig. 10, we further report the behavior of the total cross sections obtained as a sum of the contributions already shown by Fig. 5 and computed by using both the DPM and DFT potentials discussed in this work. The log scale for the cross sections in the upper right-hand panel helps us to better see the very low-energy behavior of such cross section and the very marked increase of this value

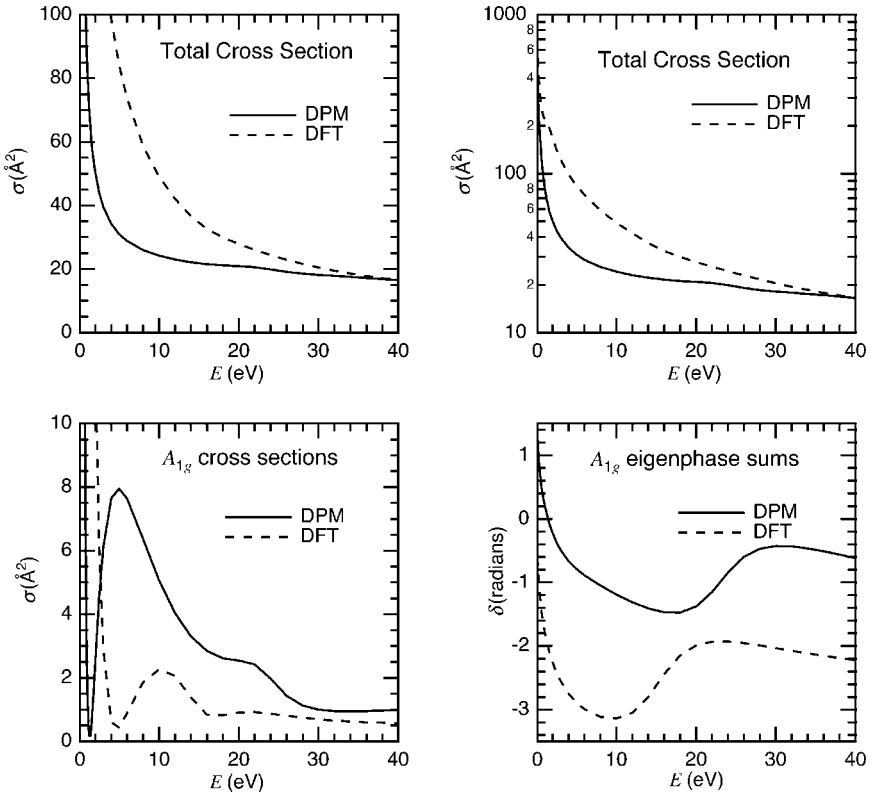

FIG. 10. Computed total cross sections (upper panels) obtained using the model interactions of the present work. Solid lines: calculations via the $V_{\mathrm{pcp}}^{\mathrm{DPM}}$; dashes: calculations via the $V_{\mathrm{pcp}}^{\mathrm{DFT}}$ potential. Lower panels: same comparison for cross section (left) and the eigenphase sum (right) for the totally symmetric contribution, A_{1g}.

as the collision energy decreases. We also see that the $V_{\mathrm{pcp}}^{\mathrm{DFT}}$ (given there by the dashed curves labeled DFT), which is the stronger of the two potentials, provides larger cross sections but does not change the general energy dependence of the cross sections. This is also confirmed by the results reported in the lower two panels, where we compare the cross sections and the eigenphase sums computed using both potential models for the A_{1g} IR contribution.

We see in the lower panel, in fact, that the shoulder around the resonance position is given by both calculations and so is the Ramsauer-Townsend minimum, although there are shifts in their location. In a similar fashion, the resonance feature of the eigenphase sum is moved to lower energies by the stronger DFT model but it remains present in the A_{1g} symmetry.

A quantitative comparison between two specific cuts of the positron-cubane interaction is reported by Fig. 11, where the direction along the C—H bond is shown for both of them: the $V_{\mathrm{pcp}}^{\mathrm{DFT}}$ is clearly much stronger in the short-range region, an area of interaction which is sampled by the lower partial waves which dominate the scattering at the lower collision energies: hence the cross-section behavior of Fig. 10. As mentioned before, it is difficult to decide which of the two potentials is more likely realistically to provide the correct interaction, although the DPM is physically more appealing and may be able in the future also to yield competitive agreement with scattering observables.

IV. GENERAL CONCLUSIONS

In this work, we have analyzed in some detail whether it would be physically possible to form temporary, metastable states of positrons trapped inside the carbon cage provided

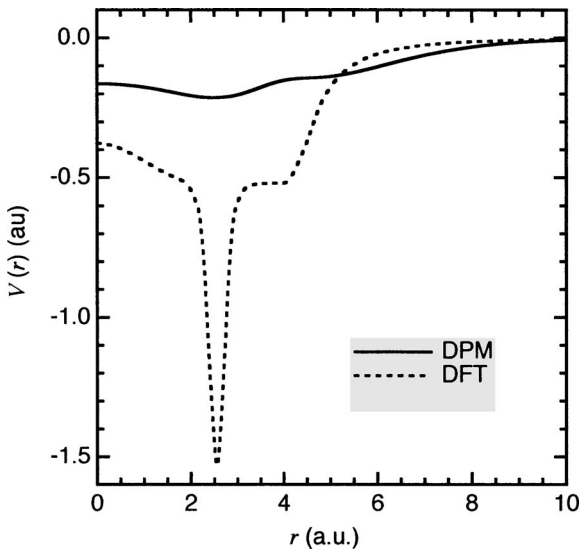

FIG. 11. Comparison of the computed V_{pcp} model potentials of the present work. The direction shown is the one along the C—H bonds from the center of mass of the cage.

by the octahedral structure of the cubane (C_8H_8) molecule in its isolated form. The motivation, besides the fundamental interest in studying the possible existence of positron-molecule complex formation in the gas phase, stems also from the potential interest related to the construction of molecular devices that can be employed to store positrons for fairly long times. In particular, carbon atom networks where the net charge inside the closed structures ("cages") is usually zero can be thought of as possible nanocontainers, whereby final bound states could be attained after complex stabilization through the extra-energy dissipation within the nuclear vibrational modes.

The system that we have studied here, however, has been considered in a preliminary stage where the nuclear motion is decoupled from the scattered positron, and therefore the chief aim here was to establish whether our theoretical models of the forces at play can suggest the presence of such metastable, trapped-positron states at relatively low energies.

We have considered two different ways in which the short-range electron-positron correlation-polarization effects, $V_{\mathrm{pcp}}(\mathbf{r}_p)$, could be included within our quantum dynamical calculations: the DPM and DFT models discussed in Sec. II. Although both models were once compared in the past by us [19,20] and have provided very similar results for elastic integral and differential cross sections for small polyatomics, we feel that to describe the positron "cloud" as a spatial entity rather than a pointlike structure is possibly a more realistic model. In the present study, we have therefore focused mainly on the results from the DPM calculations and only compared some of the final observables with those obtained when using the $V_{\mathrm{pcp}}^{\mathrm{DFT}}$ model potential. It turned out that both model treatments, although differing in the details, essentially provide the same physical picture for the process we are considering, i.e., they both indicate positron trapping inside the cage not to be very likely to occur.

The search for a trapped state has shown in fact that, although the positron-molecule interaction is essentially repulsive in the short and intermediate distances, and that fairly shallow attractive regions exist only far away from the carbon cage of the cubane, the totally symmetric component of that interaction, the A_{1g} IR, may be capable of providing a Coulomb barrier located in the region of the carbon cage and that the impinging positron can be trapped behind that barrier. It would, however, give rise to a broad metastable state at a fairly high-energy region around 20 eV. If a more realistic dynamical coupling between such a state and the nuclear vibrations could possibly be included, one would further expect that some of the metastable complex structures could decay into a finally bound state of the positron, although the competition with the cage break-up channels would also be very strong. In any event, if that stabilization channel were to survive, it could be providing a sort of nanoscopic molecular mechanism for such a positron trapping process to occur.

Another interesting property of the dynamics of positron scattering off cubane which could be compared with the behavior of electrons is the value of its scattering length, A_0, which could be obtained from [33]

$$\sigma_0 \underset{k\to 0}{\sim} 4\pi A_0^2. \tag{12}$$

The value for positron scattering is found to be positive and fairly large: 43.62 bohr, to be compared with ~ -3.4 bohr for electron scattering [9]. We therefore see that no virtual state is estimated to exist for positron scattering, as opposed to the electron scattering feature, and that the *s*-wave contribution to the cross section at low kinetic energy turns out to be fairly large.

ACKNOWLEDGMENTS

F.A.G. is grateful to the CASPUR supercomputing center for the computational support and the European Network EPIC (HPRN-CT-2002-00286) for financial support. F.A.G. and R.R.L. also acknowledge the NATO Collaborative Research Grant (2002–2005). R.R.L. wishes to acknowledge the support of the Welch Foundation (Houston, TX) for support under Grant No. A-1020.

[1] See, e.g., *New Directions in Antimatter Chemistry and Physics*, edited by C. M. Surko and F. A. Gianturco (Kluwer, Dordrecht, 2001).
[2] M. Charlton and J. M. Humbertson, *Positron Physics* (Cambridge University Press, Cambridge, 2002).
[3] H. J. Ache, *Positronium and Muonium Chemistry* (Am. Chem. Soc., Washington, DC, 1979).
[4] A. Passner, C. M. M. Surko, M. Leventhal, and A. P. Mills, Jr., Phys. Rev. A **39**, 3706 (1989).
[5] F. A. Gianturco and R. R. Lucchese, Phys. Rev. A **60**, 4567 (1999).
[6] F. A. Gianturco and R. R. Lucchese, J. Chem. Phys. **114**, 3439 (2001).
[7] F. A. Gianturco and R. R. Lucchese, Phys. Rev. A **64**, 032706 (2001).
[8] See, e.g., *Novel Aspects of Electron-Molecule Collisions*, edited by K. H. Becker (World Scientific, Singapore, 1998).
[9] F. A. Gianturco, R. R. Lucchese, A. Grandi, and N. Sanna, J. Chem. Phys. **120**, 4172 (2004).
[10] T. Nishimura and F. A. Gianturco, Phys. Rev. Lett. **90**, 1 (2003).
[11] T. Nishimura and F. A. Gianturco, Europhys. Lett. **68**, 377 (2004).
[12] F. A. Gianturco and A. Jain, Phys. Rep. **143**, 347 (1986).
[13] W. H. Press, B. P. Flannery, S. A. Teukolsky, and W. T. Vetterling, *Numerical Recipes. The Art of Scientific Computing* (Cambridge University Press, Cambridge, 1986).
[14] See, e.g., E. A. G. Armour, Phys. Rep. **169**, 1 (1988).
[15] R. N. Hewitt, C. J. Noble, and B. H. Bransden, J. Phys. B **25**, 557 (1992).
[16] M. A. Morrison, Adv. At. Mol. Phys. **24**, 51 (1988).
[17] T. L. Gibson, J. Phys. B **23**, 767 (1990).
[18] T. L. Gibson, J. Phys. B **25**, 1321 (1992).
[19] R. R. Lucchese, F. A. Gianturco, P. Nichols, and T. L. Gibson,

in *New Directions in Antimatter Chemistry and Physics*, edited by C. Surko and F. A. Gianturco (Kluwer Academic, Dordrecht, 2001), p. 475.
[20] F. A. Gianturco, T. L. Gibson, P. Nichols, R. R. Lucchese, and T. Nishimura, Radiat. Phys. Chem. **68**, 673 (2003);
[21] A. Szabo and N. Ostlund, *Modern Quantum Chemistry* (Dover, New York, 1996), p. 158.
[22] N. F. Lane, Rev. Mod. Phys. **52**, 29 (1980).
[23] A. Bouferguene, I. Ema, and C. A. Weatherford, Phys. Rev. A **59**, 2712 (1999).
[24] H. Feng, W. Sun, and M. A. Morrison, Phys. Rev. A **68**, 062709 (2003).
[25] A. Jain and F. A. Gianturco, J. Phys. B **24**, 2387 (1991).
[26] J. Arponen and E. Pajanne, Ann. Phys. (N.Y.) **91**, 450 (1975).
[27] J. Arponen and E. Pajanne, Ann. Phys. (N.Y.) **121**, 343 (1979).
[28] E. Boronski and R. M. Nieminen, Phys. Rev. B **34**, 3820 (1986).
[29] W. Kohn and L. J. Sham, Phys. Rev. **140**, A1133 (1965).
[30] R. R. Lucchese and F. A. Gianturco, Int. Rev. Phys. Chem. **15**, 429 (1996).
[31] F. A. Gianturco and R. R. Lucchese, J. Chem. Phys. **118**, 4013 (2002).
[32] F. A. Gianturco, R. Curik, R. R. Lucchese, and N. Sanna, J. Phys. B **34**, 59 (2001).
[33] C. J. Joachain, *Quantum Collision Theory* (North-Holland, Amsterdam, 1975).